

# Numerical Modeling of Polarization Gratings by Rigorous Coupled Wave Analysis

Xiao Xiang and Michael J. Escuti

Dept. Electrical and Computer Engineering, North Carolina State University, Raleigh, USA

## ABSTRACT

We report on the numerical analysis of polarization gratings (PGs) and study their general diffraction properties by using the Rigorous Coupled Wave Analysis (RCWA) method. With this semi-analytical method, we can perform rigorous simulation without paraxial approximation and have a complete understanding of diffraction behavior of PGs, including those with complex twisted layers. We first adapt the formulation of conventional RCWA to simulate grating made by anisotropic material, as appropriate for the PG profile. We then validate our RCWA method by comparing its result with that given by finite-difference time-domain (FDTD) method. Diffraction characteristics including the spectral response, angular response, and polarization dependence are investigated. A comparison of the stability and computation performance between the two methods is also briefly discussed.

**Keywords:** RCWA, polarization grating, diffraction efficiency, oblique incidence, liquid crystal

## 1. INTRODUCTION

In 1981, M. G. Moharam and T. K. Gaylord proposed a semi-analytical method to solve scattering from periodic dielectric structures.<sup>1</sup> In this Fourier-space method, devices and fields are expanded as a sum of spatial harmonics and the transmittance and reflectance is solved by calculating the electromagnetic eigenmodes. The method became known as the Rigorous Coupled Wave Analysis (RCWA), and has proven a very powerful tool for modeling of diffraction gratings. Being a semi-analytical method, RCWA is capable of simulating periodic structures for oblique incidence accurately and efficiently which can be difficult for purely numerical methods. Over the years, there have been many improvements upon the basic RCWA algorithm, aiming to implement the method in a more stable and efficient way compared to the scattering matrix<sup>2</sup> implementation. Some developments, such as algorithms based on enhanced transmittance matrices<sup>3</sup> and H matrices<sup>4</sup> have been reported and allow for more stable and faster computation.

Since first reported,<sup>5,6</sup> polarization gratings (PG) have become a distinct and important category of diffraction grating. Different from conventional phase gratings, PGs manipulate the geometric phase<sup>7</sup> and are able to diffract 100% of incident light into a single order for a certain polarization state. These unique optical properties make PGs useful for numerous applications in various fields<sup>8-10</sup> and also encourage us to predict the performance by numerical simulation.

In previous works about PG simulation, several methods have been applied, including extended Jones matrix<sup>11</sup> and FDTD.<sup>12</sup> However, in many cases they are computationally inefficient, i.e., they require long simulation times, because they can require a large number of sub-layers or a large number of points on a spatial grid. In this work, we apply the anisotropic multi-layer RCWA method in the numerical modeling PGs. Because our RCWA method is based on the enhanced transmittance matrix algorithm, it can provide accurate results much more efficiently without approximation and stability issues.

## 2. BACKGROUND

### 2.1 RCWA Review

Figure 1 shows the problem space for RCWA simulation of a generic (isotropic) surface-relief grating. The source is a plane wave excited in the entire  $x-y$  plane that propagates in the  $z$  direction. In RCWA, a grating is divided into layers that are each uniform in the  $z$  direction. The eigenmodes of electric and magnetic fields in each layer are calculated and analytically propagated. The problem is then solved by matching boundary conditions at each interface with a technique like scattering matrices, enhanced transmittance matrices or H matrices.

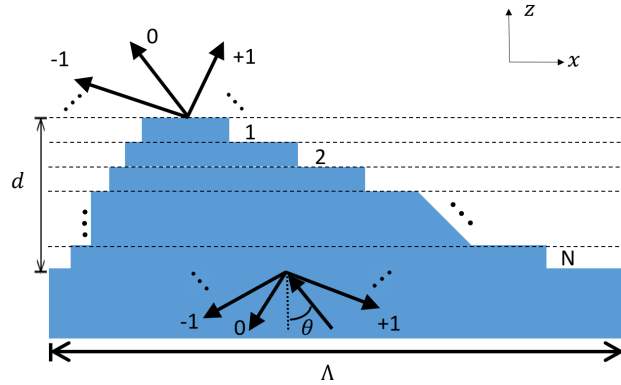


Figure 1. Geometry for a generic (isotropic) surface-relief grating. Transmitted and reflected diffraction orders are also shown.

## 2.2 Polarization Gratings

Polarization gratings comprise a periodic profile of spatially varying optical anisotropy, with spatially constant magnitude. More specifically, profiles with an in-plane optic axis that varies linearly with position. When liquid crystals are used to embody a PG, the optic axis is the same as their nematic director field, with a possible azimuthal orientation angle within a single layer following

$$\Phi(x, z) = \pi x/\Lambda + \phi z/d, \quad (1)$$

where  $\Lambda$  and  $d$  are the grating period and thickness respectively. The angle  $\phi$  represents the twist angle in the grating caused by the chiral dopants as shown in Figure 2. Two or more layers with potentially different  $d$  and  $\phi$  may be created as a monolithic film,<sup>13</sup> often to beneficially control spectrum or viewing angle behavior.

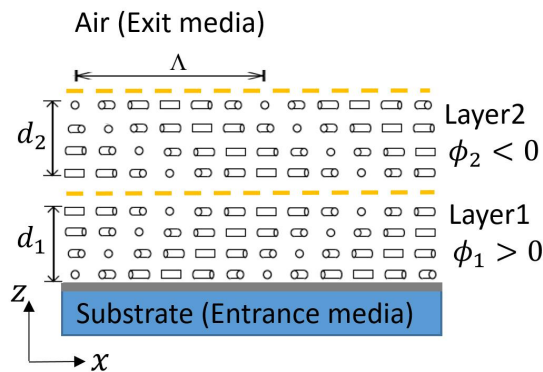


Figure 2. The structure of a typical two-twist achromatic PG. QUESTION: does this Fig. 2 correctly represent the algorithm? i.e., the user defines layer 1 and 2 from substrate up, and then the simulation has light incident from layer 2 into 1 into the substrate? If so, this would be best.]]

Conventional PGs have no twist ( $\phi = 0$ ), and can be formed by single reactive liquid crystal layer on a holographically exposed photo-alignment layer.<sup>7,14</sup> This leads to a relatively narrow high efficiency diffraction bandwidth, roughly matching a single LED color. Beyond this, high diffraction efficiency for a broadband source can be achieved using a multi-twist PG,<sup>15</sup> fabricated by adding chiral dopants into two or more different layers of the grating.

## 3. APPROACH

Different from other pure numerical methods, such as Finite-difference Time-domain, RCWA is a semi-analytical method in Fourier-space and all information about devices and fields is represented by a sum of spatial harmonics.

Given this, RCWA turns out to be very efficient to obtain diffraction efficiencies for various gratings especially when few harmonics are needed. In order to apply RCWA to periodic anisotropic structure, we first need to give a new set of core equations.

Propagation of light in source-free anisotropic dielectric media is governed by Maxwell equations and constitutive equations.

$$\nabla \times \mathbf{E} = -\frac{\partial \mathbf{B}}{\partial t} \quad (2)$$

$$\nabla \times \mathbf{H} = \frac{\partial \mathbf{D}}{\partial t} \quad (3)$$

$$\mathbf{D} = \epsilon_0 \tilde{\epsilon} \mathbf{E} \quad (4)$$

$$\mathbf{B} = \mu_0 \tilde{\mu} \mathbf{H} \quad (5)$$

The tilde signifies a tensor and  $\epsilon_0$  and  $\mu_0$  are the permittivity and the permeability of free space. Here we assume the media to be nonmagnetic and thus the  $\tilde{\mu}$  is a unity matrix. Following an improved RCWA formulation,<sup>2</sup> we insert the permittivity tensor into the curl equations and expand fields into Fourier series. For simplicity, here we assume the incidence wave vector  $\mathbf{k}_i = k_{x0}\hat{x} + k_{z0}\hat{z}$  ( $k_0 = \|\mathbf{k}_i\|$ ) and just expand the fields in the x direction:

$$E_i(x, z) = \sum_{m=-\infty}^{\infty} S_i(m; z) e^{-jk_x(m)x} \quad (6)$$

$$\bar{H}_i(x, z) = \sum_{m=-\infty}^{\infty} U_i(m; z) e^{-jk_x(m)x} \quad (7)$$

$$\epsilon_{ij}(x) = \sum_{m=-\infty}^{\infty} c_{ij}(m) e^{-jKx} \quad (8)$$

where subscripts  $i, j$  represent components in  $x, y, z$  directions and  $k_x(m) = k_{x0} - 2\pi m/\Lambda$ . Note that  $\bar{H}_i = -j\sqrt{\mu_0/\epsilon_0}H_i$  are the normalized components of magnetic field. After substituting Equation (6) and (7) into (2)-(5) and proper simplification, we get the following equations in the matrix form.

$$\frac{d\mathbf{s}_y}{d\bar{z}} = -\mathbf{u}_x \quad (9)$$

$$\frac{d\mathbf{s}_x}{d\bar{z}} + j\bar{k}_x \mathbf{s}_z = -\mathbf{u}_y \quad (10)$$

$$-j\bar{k}_x \mathbf{s}_y = \mathbf{u}_z \quad (11)$$

$$\frac{d\mathbf{u}_y}{d\bar{z}} = -\tilde{\epsilon}_{xx} \mathbf{s}_x - \tilde{\epsilon}_{xy} \mathbf{s}_y \quad (12)$$

$$\frac{d\mathbf{u}_x}{d\bar{z}} + j\bar{k}_x \mathbf{u}_z = \tilde{\epsilon}_{yx} \mathbf{s}_x + \tilde{\epsilon}_{yy} \mathbf{s}_y \quad (13)$$

$$-j\bar{k}_x \mathbf{u}_y = \tilde{\epsilon}_{zz} \mathbf{s}_z \quad (14)$$

Here  $\mathbf{s}_{x,y,z}$  and  $\mathbf{u}_{x,y,z}$  are vectors of corresponding mode coefficients. For example,  $\mathbf{s}_x = [S_x(m = -M), S_x(m = -(M-1)), \dots, S_x(m = M)]^T$ , noting that we already truncate the number of modes to be  $2M+1$  and  $\bar{z} = z/k_0$ ,  $\bar{k}_x = k_x/k_0$  are the normalized variables. Given the expansion of permittivity in (8), the convolution matrix is determined by  $\tilde{\epsilon}_{ij}(m, n) = c_{ij}(n-m)$ .

Due to the fact that the director profile of PG is a linear function of space, we can easily write it in terms of Fourier series as shown in (15) and (16). Assuming zero pretilt in the grating, the permittivity of PG with period  $\Lambda$  is given by:<sup>12</sup>

$$\tilde{\epsilon} = \tilde{\epsilon}_0 + \tilde{\epsilon}_1 = \begin{pmatrix} b & 0 & 0 \\ 0 & b & 0 \\ 0 & 0 & n_0^2 \end{pmatrix} + a \begin{pmatrix} \cos(Kx) & \sin(Kx) & 0 \\ \sin(Kx) & -\cos(Kx) & 0 \\ 0 & 0 & 0 \end{pmatrix} \quad (15)$$

where  $a = (n_o^2 - n_e^2)/2$  and  $b = (n_o^2 + n_e^2)/2$ . Here,  $n_o$  and  $n_e$  are the indices of refraction of ordinary and extraordinary light respectively. The modulated part  $\tilde{\epsilon}_1$  can be further written into

$$\tilde{\epsilon}_1 = \frac{a}{2} \begin{pmatrix} 1 & -j & 0 \\ -j & -1 & 0 \\ 0 & 0 & 0 \end{pmatrix} e^{jKx} + \frac{a}{2} \begin{pmatrix} 1 & j & 0 \\ j & -1 & 0 \\ 0 & 0 & 0 \end{pmatrix} e^{-jKx} \quad (16)$$

From equation (15) and (16), we can clearly see that there are only three terms in the expansion of permittivity tensor in Fourier-space. This implies that the grating will respond to three eigenmodes of the incidence fields and the output fields will be the superposition of these eigenmodes, which results in the unique polarization dependence of PG. Therefore, the zero-order will have the same polarization state as the incidence wave while the first-orders will be left and right circular polarized as shown in Figure 3 (b).

Given the expansion, we can further determine the convolution matrix related to the permittivity tensor. Following the enhanced transmittance matrix algorithm,<sup>3</sup> the mode coefficients of transmitted and reflected waves are solved by matching all boundary conditions at each interfaces. The transmittance, reflectance and diffraction efficiency of each order are calculated from corresponding mode coefficients at the last step of the simulation.

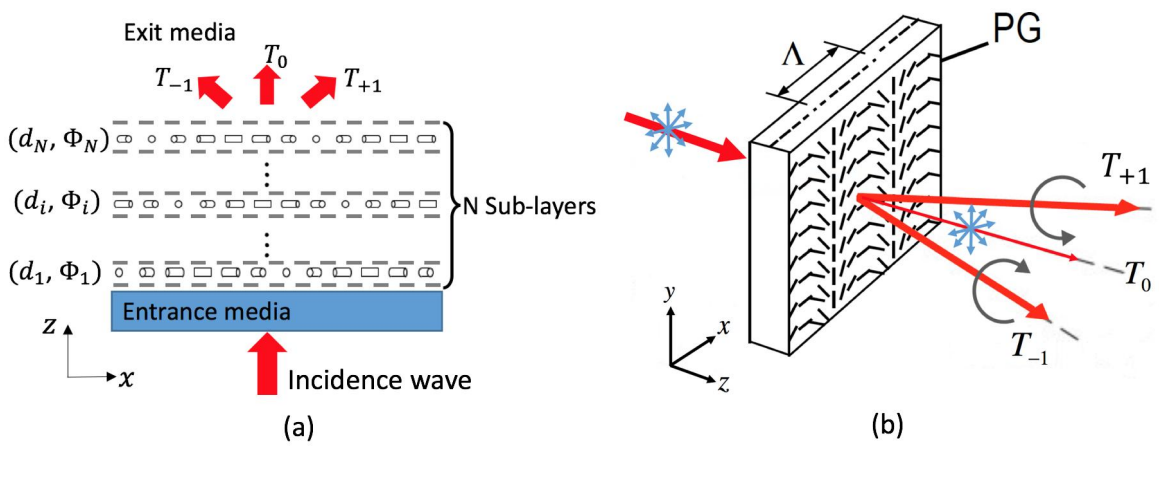


Figure 3. (a) Illustration of  $N$  sub-layers for a multi-two-twist, (b) Polarization dependence of diffraction orders.

For the case where permittivity varies in  $z$  direction, such as the multi-twist PG, a multi-layer RCWA method is required. Similar to the case of surface-relief grating, we further divide the each layer  $(d_j, \phi_j)$  of the grating in Figure 2 into 10 to 40 thin sub-layers  $(d_i, \Phi_i)$  as shown in Figure 3 (a). In each sub-layer, we assume the permittivity tensor is uniform in  $z$  direction and thus can be determined by a corresponding azimuthal orientation angle  $\Phi_i$  of that sub-layer. Then we rewrite the modulated part of permittivity as

$$\tilde{\epsilon}_1 = a \begin{pmatrix} \cos[2\Phi(x, z)] & \sin[2\Phi(x, z)] & 0 \\ \sin[2\Phi(x, z)] & -\cos[2\Phi(x, z)] & 0 \\ 0 & 0 & 0 \end{pmatrix}$$

where  $\Phi(x, z)$  can be determined from Equation (1) for each sub-layer in the grating to get the corresponding permittivity tensor. With all permittivity tensors determined, we match all boundary conditions for every interface between sub-layers, which basically follows the same approach as that in the single layer case. Note that enough sub-layers are needed to simulate a multi-twist PG accurately, especially when the twist angle is large in the grating.

## 4. RESULTS

### 4.1 Simulation Results

Since the anisotropic grating will inherently change the polarization state of the incident light, our RCWA method is designed to support any polarization state. For validation, we consider the spectral and angular response of two PGs of different types. The first grating is chosen to be a non-twist type and has period  $\Lambda = 6.5\mu\text{m}$ , thickness  $d = 1.7\mu\text{m}$ , birefringence  $\Delta n = 0.16$  and average index  $\bar{n} = 1.6$ . The other PG is known as a two-twist achromatic PG,<sup>15</sup> opposite twist is induced in the grating by adding chiral dopants. Each layer has the same thickness as the first PG and other parameters are also the same. The incident wave is set to be right circularly polarized for both polarization gratings. The simulation results are shown in Figure 4 and 5 compared to the simulation given by FDTD.

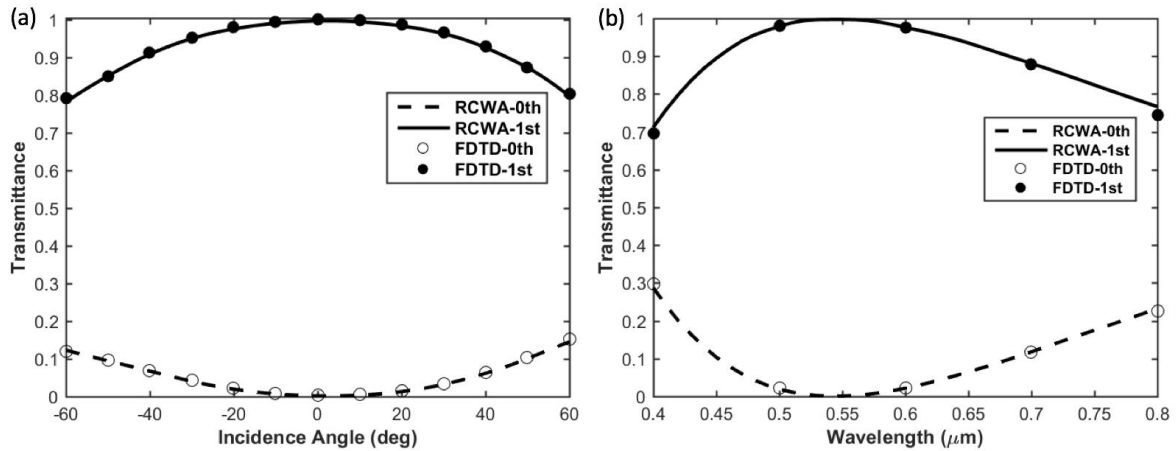


Figure 4. (a) Angular response of non-twist PG at 532nm, (b) Spectral response of non-twist PG at normal incidence.

Generally, for a typical non-twist PG, the peak of the efficiency curve occurs at the normal incidence. The minor decrease in efficiency at large incident angle is mainly caused by the deviation from the half-wave retardation condition as shown in Figure 5 (a). Depending on the birefringence and thickness, this deviation can be large but typically high efficiency can be preserved when the incidence angle is less than 30 degrees. From Figure 5 (b), the peak of first-order transmittance is located at the optimal 544nm wavelength given the thickness and birefringence. The wavelength dependence for normal incidence can be also predicted from analytical results based on paraxial approximation.<sup>16</sup>

The angular response is similar to the non-twist version as shown in Figure 5 (a). Although the drop of efficiency at large incidence angle seems to be more significant, it is still capable to provide good response within the range of 30 degrees. For the achromatic PG simulated here, we expect a improvement in its wide-band performance. From the result in Figure 5 (b), both simulation methods predict a high broadband efficiency which is in good agreement with the experimental work in Ref.<sup>15</sup> The two-twist achromatic PG indeed shows a great enhancement in wide-band efficiency compared to the non-twist PG. Actually, more complex and effective designs<sup>13</sup> have been shown to provide high diffraction efficiency for even wider bandwidths in the visible and infrared ranges.

### 4.2 Stability and Performance

We implement the RCWA following the well known enhanced transmittance matrix algorithm. Compared to the traditional scattering matrix method, the ETM avoids the instability caused by matrix inversion and reduces the matrix calculations which improves the performance greatly. However, for FDTD, the stability problem needs to be carefully taken care of especially at large incidence angles.

For a conventional surface-relief grating, we usually need to keep dozens of spatial harmonics to get convergent and accurate results, which certainly slows down the calculation. Note that the expansion of permittivity of PG

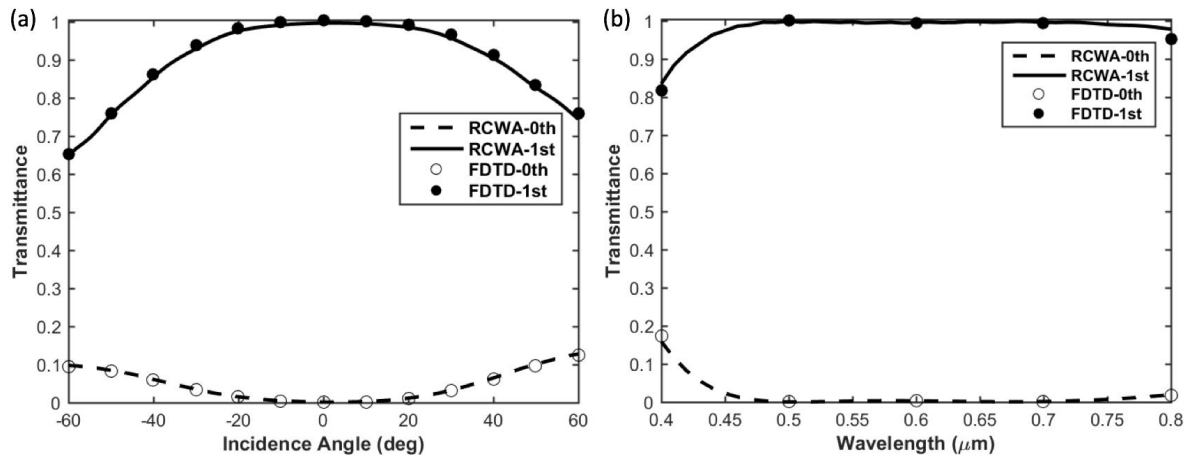


Figure 5. (a) Angular response of achromatic PG at 532nm, (b) Spectral response of achromatic PG at normal incidence.

just yields three terms, which implies we can get accurate result with just several modes. Given the simplicity in Fourier-space, RCWA has shown great advantages in diffraction efficiency calculation for PGs and overwhelms FDTD method significantly. For example, the FDTD method may need 1 2 minutes to calculate each data point in Figure 4(a) on a modern laptop or desktop computer, while the RCWA is capable to obtain the whole efficiency curve in 1 2 seconds.

## 5. CONCLUSIONS

In this work, we first modify and apply the RCWA method to simulate in-plane varying anisotropic gratings and perform a rigorous numerical analysis of the non-twist/multi-twist PGs. The diffraction behavior is mainly viewed from angular and wavelength response of the grating. We validate the tool by comparing the results with the existing FDTD method. The RCWA method shows great advantage in stability and performance for diffraction efficiency calculation, typically more than fifty times faster than the FDTD simulation.

## ACKNOWLEDGMENTS

The authors acknowledge the financial support of ImagineOptix Corporation, within which MJE holds an equity interest.

## REFERENCES

- [1] Moharam, M. G. and Gaylord, T. K., "Rigorous coupled-wave analysis of planar-grating diffraction," *J. Opt. Soc. Am. A* **71**, 811–818 (1981).
- [2] Rumpf, R. C., "Improved formulation of scattering matrices for semi-analytical methods that is consistent with convention," *Progress In Electromagnetics Research B* **35**, 241–261 (2011).
- [3] Moharam, M. G., Gaylord, T. K., Pommet, D. A., and Grann, E. B., "Stable implementation of the rigorous coupled-wave analysis for surface-relief gratings: enhanced transmittance matrix approach," *J. Opt. Soc. Am. A* **12**, 1077–1086 (1995).
- [4] Tan, E. L., "Hybrid-matrix algorithm for rigorous coupled-wave analysis of multilayered diffraction gratings," *Journal of Modern Optics* **53**, 417–428 (2006).
- [5] Todorov, T., Nikolova, L., Stoyanova, K., and Tomova, N., "Polarization holography. 3: Some applications of polarization holographic recording," *Appl. Opt.* **25**, 785–788 (1985).
- [6] Eakin, J. N., Xie, Y., Pelcovits, R. A., Radcliffe, M. D., and Crawford, G. P., "Zero voltage Fredericksz transition in periodically aligned liquid crystals," *Appl. Phys. Lett.* **85**, 1671 (2004).
- [7] Kim, J., Li, Y., Miskiewicz, M. N., Oh, C., Kudenov, M. W., and Escuti, M. J., "Fabrication of ideal geometric-phase holograms with arbitrary wavefronts," *Optica* **2**, 958–964 (2015).

- [8] Komanduri, R. K., Oh, C., and Escuti, M. J., "Polarization independent projection systems using thin film polymer polarization gratings and standard liquid crystal microdisplays," *SID Symp. Dig. Tech. Papers* **40**, 487–490 (2009).
- [9] Kudenov, M., Escuti, M., Hagen, N., Dereniak, E., and Oka, K., "Snapshot imaging Mueller matrix polarimeter using polarization gratings," *Opt. Lett.* **37**, 1367–1369 (2012).
- [10] Kim, J., Oh, C., Serati, S., and Escuti, M. J., "Wide-angle, nonmechanical beam steering with high throughput utilizing polarization gratings," *Appl. Opt.* **50**, 2636–2639 (2011).
- [11] Tan, L., Ho, J. Y., and Kwok, H.-S., "Extended Jones matrix method for oblique incidence study of polarization gratings," *Appl. Phys. Lett.* **101**, 051107 (2012).
- [12] Oh, C. and Escuti, M. J., "Time-domain analysis of periodic anisotropic media at oblique incidence: an efficient FDTD implementation," *Opt. Express* **14**, 11870–11884 (2006).
- [13] Komanduri, R. K., Lawler, K. F., and Escuti, M. J., "Multi-twist retarders: broadband retardation control using self-aligning reactive liquid crystal layers," *Optics Express* **21**, 404–420 (2013).
- [14] Crawford, G. P., Eakin, J. N., Radcliffe, M. D., Callan-Jones, A., , and Pelcovits, R. A., "Liquid-crystal diffraction gratings using polarization holography alignment techniques," *J. Appl. Phys.* **98**, 123102 (2005).
- [15] Oh, C. and Escuti, M. J., "Achromatic diffraction from polarization gratings with high efficiency," *Opt. Lett.* **33**, 2287–2289 (2008).
- [16] Oh, C. and Escuti, M. J., "Numerical analysis of polarization gratings using the finite-difference time-domain method," *Phys. Rev. A* **76**, 043815 (2007).